

Plasmon stimulated emission in arrays of bimetallic structures coated with dye-doped dielectric

A. Krishnan,¹ S. P. Frisbie,¹ L. Grave de Peralta,² and A. A. Bernussi^{1,a)}

¹Department of Electrical and Computer Engineering and Nano Tech Center, Texas Tech University, Lubbock, Texas 79409, USA

²Department of Physics and Nano Tech Center, Texas Tech University, Lubbock, Texas 79409, USA

(Received 30 December 2009; accepted 19 February 2010; published online 15 March 2010)

We report results on the propagation modes in plasmonic structures incorporating a gain medium using Fourier-plane leakage radiation microscopy. We demonstrate that high contrast images and detailed mode propagation information can be obtained with arrays of dielectric loaded surface plasmon waveguides. Clear interference effects were observed in the Fourier-plane images corresponding to arrays of bimetallic stripes coated with a gain material. This indicates coherent superposition of leaked fluorescence from coupled adjacent waveguides as a result of plasmon stimulated emission. © 2010 American Institute of Physics. [doi:10.1063/1.3361654]

Light confinement and manipulation at the nanoscale is a key requirement to realize ultracompact photonic devices and integration of optics with microelectronics. Surface plasmon polaritons (SPPs) confined along metal-dielectric interfaces provide a definite path to accomplish this goal.^{1,2} Recently, several approaches have been reported addressing the design, fabrication, and characterization of SPP structures with subwavelength dimensions.²⁻⁶ However, the intrinsic losses in SPP waveguides prevent light propagation over long distances. In order to overcome this issue, the integration of an active gain media with SPP waveguides has been proposed to simultaneously achieve light confinement in the nanoscale and compensate for propagation losses.^{5,7} The addition of a dielectric gain medium close to the metal layer has also attracted considerable interest for realization of plasmon lasers operating at optical frequencies. Demonstration of plasmon stimulated emission is a fundamental step to obtain SPP based lasers and several reports have been dedicated to this effort.⁸⁻¹²

Leakage radiation microscopy (LRM) is a recently developed imaging technique that relies on the leakage of surface plasmon mode into the substrate.⁶ LRM provides raster free images along with the capability of Fourier plane imaging. Recently, SPP coupled fluorescence has been used to minimize the effects of the direct incident beam, thus improving considerably the image contrast obtained by LRM.^{9,13} Furthermore, the approach is relatively easy to implement and cost effective, particularly when compared with methods such as near-field scanning optical microscopy. However, no detailed investigation demonstrating stimulated emission using Fourier-plane LRM (FP-LRM) has been reported.

In this paper, we investigate the propagation modes in periodic arrays of dielectric loaded SPP waveguides and bimetallic stripes (BMS) coated with a gain medium using Fourier-plane LRM. We demonstrate that using an array of waveguides instead of a single waveguide results in well-defined FP-LRM images providing detailed information about the propagation modes. High contrast FP-LRM images on arrays of BMSs show clear interference effects which

demonstrate the occurrence of plasmon stimulated emission.

Figure 1 shows the schematic of the two SPP structures investigated here. They are comprised of periodic arrays of dielectric loaded SPP waveguides (DLSPW) (Ref. 6) and BMSs. Both structures were fabricated with identical period (p) and stripe width (w) parameters. The DLSPW sample in Fig. 1(a) consists of an array of dielectric waveguides doped with rhodamine 6G (R-6G).^{3,6} The sample was fabricated on a glass substrate covered with ~ 50 nm thick gold layer. A 100 nm thick polymethylmethacrylate (PMMA) doped with R-6G was spin coated over the gold layer. The doped PMMA layer was patterned using e-beam lithography. BMS samples in Fig. 1(b) also consist of a glass substrate covered with a 50 nm thick gold layer. PMMA was spin coated over the gold layer and the ridges were also defined using e-beam lithography. A 65 nm thick aluminum layer was then evaporated and lifted-off to define the BMSs. Finally, a 100 nm thick PMMA layer doped with R-6G, with characteristics identical to that one used to fabricate the DLSPW sample depicted in Fig. 1(a), was spin coated over the entire patterned sample. It is worth mentioning here that in the case of DLSPW samples the width of the waveguides corresponds to the width of the PMMA-R-6G stripes while the width of the waveguides in the BMS samples corresponds to the width of the gold region which is not covered by the aluminum layer, see Fig. 1(b). We fabricated two different sets of SPP samples. In each set the width of the waveguide was fixed to $w=1 \mu\text{m}$ but two different periods were used: p

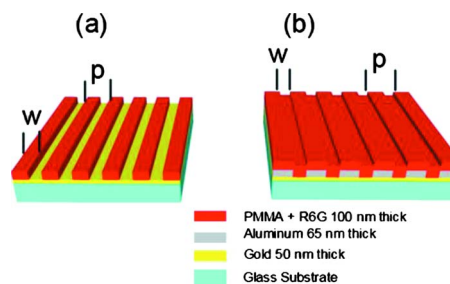


FIG. 1. (Color online) Schematic (not to scale) of fabricated structures consisting of arrays of (a) R-6G doped DLSPW and (b) R-6G coated BMS.

^{a)}Electronic mail: ayrtan.bernussi@ttu.edu.

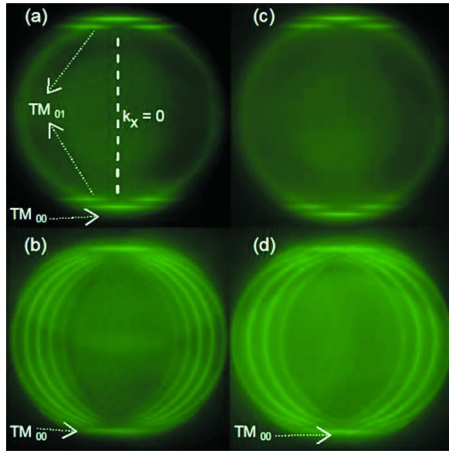


FIG. 2. (Color online) FP-LRM images of arrays of (a) DLSPPW ($p=4 \mu\text{m}$), (b) BMS ($p=4 \mu\text{m}$), (c) DLSPPW ($p=3 \mu\text{m}$), and (d) BMS ($p=3 \mu\text{m}$). In all samples $w=1 \mu\text{m}$ were used.

$=3 \mu\text{m}$ and $p=4 \mu\text{m}$. On both types of samples the patterned area was $200 \times 200 \mu\text{m}^2$.

All samples were investigated by LRM. A continuous wave diode laser emitting at 532 nm wavelength was used as the excitation source. Illumination was performed through the patterned side of the samples using a laser beam spot area of $\sim 1 \text{ mm}^2$ with $\sim 2 \text{ mW}$ power. Since our method utilizes multiple waveguides, it is not essential to utilize precise focusing optics, normally required to excite single SPP waveguides.^{6,9} This simplifies the optical setup implementation while providing superior image contrast in the Fourier plane due to the contribution of the leaked modes from the multiple waveguides. The leakage radiation was imaged from the glass substrate with the aid of an immersion oil microscope objective with a high numerical aperture ($\text{NA}=1.3$) placed in close contact with the sample.¹³ A band pass filter centered at $\sim 566 \text{ nm}$ wavelength was used to block the direct laser beam and to allow the transmission of R-6G SPP waveguide coupled fluorescence. A lens-CCD camera arrangement was used to image the Fourier plane of the patterned samples.

Figures 2(a) and 2(b), respectively, show the FP-LRM images of arrays of DLSPPW and BMS samples with $w=1 \mu\text{m}$ and $p=4 \mu\text{m}$. The FP-LRM images of plasmonic structures correspond to a map of the SPP propagation momentum. The weak background in Fig. 2(a) is due to a small amount of R-6G fluorescence that is transmitted directly through the thin metal layer without plasmon-coupling. The radius of the background disk corresponds to the maximum collection angle of the leakage radiation by the microscope objective lens.¹³ The horizontal emission line segments observed in Fig. 2(a), occurring along the wave vector (k) in the y -direction (i.e., $k_x=0$), correspond to the fundamental and the first excited modes within the waveguide. The effective refractive indexes of the propagating modes can be determined from the ratio between the radii of the emission lines and the radius of the maximum collecting angle from the high NA lens.⁶ The outermost horizontal line segment corresponds to the fundamental transverse magnetic waveguide mode (TM_{00}) with effective refractive index of ~ 1.15 . The inner horizontal line segment has an effective refractive index of ~ 1.08 and corresponds to the first TM_{01} mode. The line segment corresponding to the TM_{01} mode has a clear

interruption at $k_x=0$, which indicates that this waveguide mode cannot be excited by incident light parallel to the waveguide. Hence, this corresponds to an odd mode. On the other hand, the line segment corresponding to the TM_{00} is continuous at $k_x=0$ and therefore corresponds to an even mode which can be excited by incident light parallel to the waveguide. Figure 2(b) shows the FP-LRM image corresponding to an array of BMS with $w=1 \mu\text{m}$ and $p=4 \mu\text{m}$. Similar to the FP-LRM image of the DLSPPW sample, the signature of the TM_{00} guided mode (effective refractive index of ~ 1.1) at the image edges along $k_x=0$, can be also clearly observed in Fig. 2(b). However, in contrast to Fig. 2(a), interference fringes in the form of a set of periodic rings are clearly visible in the FP-LRM image of the BMS sample. The observed interference features are experimental evidence of the occurrence of plasmon stimulated emission in the BMS structure. Due to the continuous layer of PMMA-R-6G, Fig. 1(b), SPP excitation is weakly coupled to the waveguides in the BMS sample. This results in lateral coupling between adjacent waveguides. Consequently, the interference pattern observed in Fig. 2(b) results from a coherent superposition of plasmon coupled fluorescence leaked from different waveguides in the BMS sample. In the case of DLSPPW, the emission from adjacent stripes of PMMA-R6G has no phase coherence due to the discontinuity in the gain medium and due to the strong localization of the guided modes in this type of waveguide. The leakage radiation from adjacent waveguides yields no visible interference pattern in Fig. 2(a) due to the lack of coherence.

In order to verify the hypothesis of plasmon stimulated emission, another set of samples consisting of arrays of DLSPPW and BMS were fabricated with a different period. Figure 2(c) shows the FP-LRM image corresponding to an array of DLSPPW stripes with $w=1 \mu\text{m}$ and $p=3 \mu\text{m}$. Similarly to Fig. 2(a), the continuous and interrupted line segments in the FP-LRM image of this sample correspond to the TM_{00} and TM_{01} waveguide modes, respectively. As anticipated, the FP-LRM image of the DLSPPW sample with $p=3 \mu\text{m}$ also shows no evidence of interference fringes. Figure 2(d) shows the FP-LRM image corresponding to an array of BMS with $w=1 \mu\text{m}$ and $p=3 \mu\text{m}$. As can be clearly seen, the separation between consecutive fringes increased when compared to the BMS sample with $p=4 \mu\text{m}$ in Fig. 2(b). We determined an increase of fringe separation by a factor of ~ 1.3 . This change in interference fringe periodicity is consistent with the decrease in the waveguide separation from 4 to 3 μm , confirming the occurrence of coherence of plasmon coupled fluorescence leaked from different waveguides.

In conclusion, we have observed interference effects in the FP-LRM images of arrays of BMSs coated with PMMA-R-6G. The origin of the interference fringes is attributed to coherent superposition of plasmon coupled fluorescence leaked from weakly coupled waveguides. Our results revealed that the separation between fringes varies inversely with the period of the stripes, confirming the coherent nature of the periodic features observed in the FP-LRM images of the BMS samples. We anticipate that this type of structure can be potentially used in the realization of plasmonic interference based devices and lasers. We have also demonstrated that using arrays of dielectric loaded plasmonic waveguides result in superior contrast FP-LRM images when compared to single waveguides. This allowed us to obtain detailed in-

formation about the mode type and mode order and its corresponding effective refractive index.

This work is partly supported by the U.S. Army CERDEC Contract (W15P7T-07-D-P040) and the J. F Maddox Foundation.

- ¹S. A. Maier, P. G. Kik, H. A. Atwater, S. Meltzer, E. Harel, B. E. Koel, and A. A. G. Requicha, *Nature Mater.* **2**, 229 (2003).
²R. Zia, M. D. Selker, P. B. Catrysse, and M. L. Brongersma, *J. Opt. Soc. Am.* **21**, 2442 (2004).
³T. Holmgaard, S. I. Bozhevolnyi, L. Markey, and A. Dereux, *Appl. Phys. Lett.* **92**, 011124 (2008).
⁴J. A. Dionne, L. A. Sweatlock, H. A. Atwater, and A. Polman, *Phys. Rev. B* **73**, 035407 (2006).

- ⁵A. Krishnan, L. G. de Peralta, M. Holtz, and A. A. Bernussi, *J. Lightwave Technol.* **27**, 1114 (2009).
⁶J. Grandidier, S. Massenot, G. Colas des Francs, A. Bouhelier, J.-C. Weeber, L. Markey, A. Dereux, J. Renger, M. U. González, and R. Quidant, *Phys. Rev. B* **78**, 245419 (2008).
⁷M. P. Nezhad, K. Tetz, and Y. Fainman, *Opt. Express* **12**, 4072 (2004).
⁸D. J. Bergman and M. I. Stockman, *Phys. Rev. Lett.* **90**, 027402 (2003).
⁹J. Grandidier, G. Colas des Francs, S. Massenot, A. Bouhelier, L. Markey, J. C. Weeber, C. Finot, and A. Dereux, *Nano Lett.* **9**, 2935 (2009).
¹⁰O. Popov, V. Lirtsman, and D. Davidov, *Appl. Phys. Lett.* **95**, 191108 (2009).
¹¹J. Seidel, S. Grafstrom, and L. Eng, *Phys. Rev. Lett.* **94**, 177401 (2005).
¹²M. A. Noginov, G. Zhu, M. Mayy, B. A. Ritzo, N. Noginova, and V. A. Podolskiy, *Phys. Rev. Lett.* **101**, 226806 (2008).
¹³S. P. Frisbie, C. F. Chesnutt, M. E. Holtz, A. Krishnan, L. Grave de Peralta, and A. A. Bernussi, *IEEE Photonics Journal* **1**, 153 (2009).